THE
PHYSICAL REVIEW

A journal of experimental and theoretical physics established by E. L. Nichols in 1893

SECOND SERIES, Vol. 136, No. 1A 5 OCTOBER 1964

Spectral Properties of a Single-Mode Ruby Laser: Evidence of Homogeneous Broadening of the Zero-Phonon Lines in Solids*

C. L. TANG, H. STATZ, G. A. DEMARS, AND D. T. WILSON
Raytheon Research Division, Waltham, Massachusetts
(Received 27 April 1964)

According to several recent studies, the width of the sharp zero-phonon lines in the electronic spectra of impurities in solids, such as the R lines of ruby, is due to Raman scattering of phonons by the impurity ions. The question whether such zero-phonon lines are homogeneously broadened is an important one, both for its own interest and for optical-maser applications. From a detailed study of the stimulated-emission spectra of a ruby laser operating in the traveling-wave modes, we obtain conclusive evidence that such zero-phonon lines are homogeneously broadened. Because the R_1 line of ruby is essentially homogeneously broadened at room temperature, the traveling-wave laser oscillates for all practical purposes only in a single mode. The spectral width of the laser emission is extremely sharp. It is less than 0.005 cm^{-1} at room temperature as compared to a width of the order of 1 cm^{-1} for conventional ruby lasers of comparable intensity. In addition, the output intensity no longer shows random spikes but shows a predictable train of regularly spaced spikes which agree well with theory.

I. INTRODUCTION

THE unique properties of various types of optical masers[1] have made it possible to do a number of new experiments and to observe many new effects. For example, the unusual stability and spectral purity of the gas laser[2] permits one to use it for certain precision measurements, and the powerful outputs of the solid-state lasers[3] have led to the observations of many new higher order effects. Unfortunately, the total spectral widths of most high-power lasers, such as the Nd-doped glass laser[4] and the ruby laser, are quite broad. Conventional Nd-doped glass lasers have a total spectral width of the order of 50 cm^{-1}; specially designed Nd glass lasers have been reported to have a width of the order of 1 cm^{-1}.

In the case of ruby, at room temperature the width of the R_1 fluorescence line is of the order of 10 cm^{-1} or more. Within this linewidth there can be many resonances of the Fabry-Perot cavity used in the maser; these resonances are separated in wave numbers by $1/2L$ for the longitudinal modes where L is the total optical path between the mirrors of the Fabry-Perot cavity. It is well known that in conventional ruby lasers many of these longitudinal modes do go into oscillation simultaneously, and the total spectral width of the laser output is of the order of 1 cm^{-1} at room temperature.[5] In addition, such lasers usually have an almost random spiking output with each individual mode showing quite a different spiking pattern. These undesirable characteristics have made it difficult to make such measurements where both the intensity and the spectral purity of the laser output are important. For example, they may be responsible for some of the seemingly contradictory quantitative results obtained in recent experiments in higher order Raman effects and nonlinear effects in optics. The problem of reducing the number of oscillating modes in high-power solid-state lasers to a single mode is therefore an important one. It is not a simple problem due to the fact that the fluorescence linewidth is normally very broad compared to the separation between cavity resonances. It would be difficult to operate the laser close enough to the threshold or suitably modify the cavity resonance properties to facilitate

* Work supported in part initially by Contract No. AF 33(657)-9173, Wright-Patterson Air Force Base, Dayton, Ohio; and presently by AF 19(628)-3862, AFCRL, Hanscom Field, Bedford, Massachusetts.

[1] A. L. Schawlow and C. H. Townes, Phys. Rev. **112**, 1940 (1958).

[2] A. Javan, W. R. Bennett, Jr., and D. R. Herriott, Phys. Rev. Letters **6**, 106 (1961).

[3] T. H. Maiman, Nature **187**, 493 (1960).

[4] E. Snitzer, *Proceedings of the Third International Symposium on Quantum Electronics* (Columbia University Press, New York, 1964).

[5] C. L. Tang, H. Statz, and G. A. deMars, J. Appl. Phys. **34**, 2289 (1963).

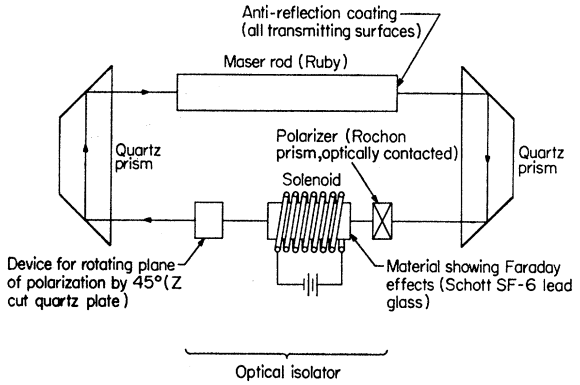

FIG. 1. Schematic diagram of experimental laser with optical isolator for obtaining traveling-wave resonant modes.

oscillation in a few modes; furthermore, these schemes would seriously limit the total power output and in our laboratory have rarely given genuine single-mode oscillation with appreciable intensity.

In a previous publication,[5] we suggested an experiment for obtaining single-mode operation of a ruby laser and reported some preliminary results.[6] We have now made a detailed study of the output characteristics of the laser. The experimental results show that considerable care must be exercised before one can be sure of single-mode oscillation, and, in our experiment, single-mode operation at a substantial power level is indeed obtained. The total spectral width is no more than 0.005 cm^{-1}. The true width is not yet known due to instrumental limitations. In addition, the laser output no longer shows random spikes but shows a predictable train of regularly spaced spikes which agree well with calculated results.

The experimental results also prove that the R_1 line of ruby is essentially homogeneously broadened at room temperature.

According to several recent studies,[7] the widths of the sharp zero-phonon lines in the electronic spectra of impurities in solids are due to Raman scattering of phonons by the impurity ions. The temperature dependence of the width and shift of the $^2E \rightarrow {}^4A_2$ transitions of V^{2+} in MgO and Cr^{3+} in MgO and Al_2O_3 has been found to be reasonably well accounted for with the help of such a model. For example, at room temperature the R_1 line of dilute ruby is primarily broadened by the two-phonon Raman process; at 77°K and below, the width appears to be dominated by strain broadening. The question as to whether or not such zero-phonon lines are homogeneously broadened is an important one, both for its own interest and for optical maser applications. In the present experiment, we obtain conclusive evidence that, at room temperature, one cannot "burn a hole" into the zero-phonon part of the R_1 line in ruby; therefore, such lines are homogeneously broadened.

[6] C. L. Tang, H. Statz, and G. A. deMars, Appl. Phys. Letters 2, 222 (1963).

[7] R. H. Silsbee, Phys. Rev. 128, 1726 (1962); D. E. McCumber and M. D. Sturge, J. Appl. Phys. 34, 1682 (1963); G. F. Imbush, W. M. Yen, A. L. Schawlow, D. E. McCumber, and M. D. Sturge, Phys. Rev. 133, A1029 (1964).

II. EXPERIMENTAL

The fact that the ruby laser oscillates simultaneously in many longitudinal modes implies at least one of two things: (1) The fluorescence line is inhomogeneously broadened so that any oscillating mode merely burns a hole into the fluorescence line, but does not appreciably affect the fluorescence into the other cavity modes. (2) The fluorescence line is homogeneously broadened, but there is very little spatial diffusion of the excitations of the Cr^{3+} ions. Due to the standing-wave distributions of the intensity of the oscillating modes, it is possible to "eat holes" spatially into the distribution of the inverted population of the Cr^{3+} ions and thus lead to simultaneous oscillation of many modes.

There is reason to believe that the second possibility is correct. We have investigated this possibility in considerable detail and found it to be able to account for many characteristics of the solid-state lasers. If this is indeed the case, then to achieve single-mode operation of the laser, one should avoid nonuniform de-excitation of the inverted population. For the experiment reported here, we have constructed an optical maser in which all

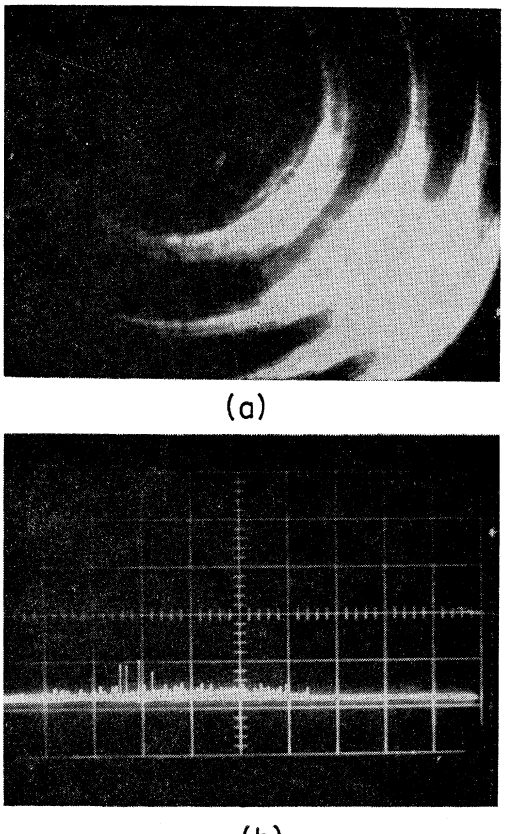

FIG. 2. (a) Fabry-Perot pattern and (b) output intensity of a conventional ruby laser at room temperature. The separation between Fabry-Perot orders is 1.6 cm^{-1}; scope scale is 100 μsec/cm.

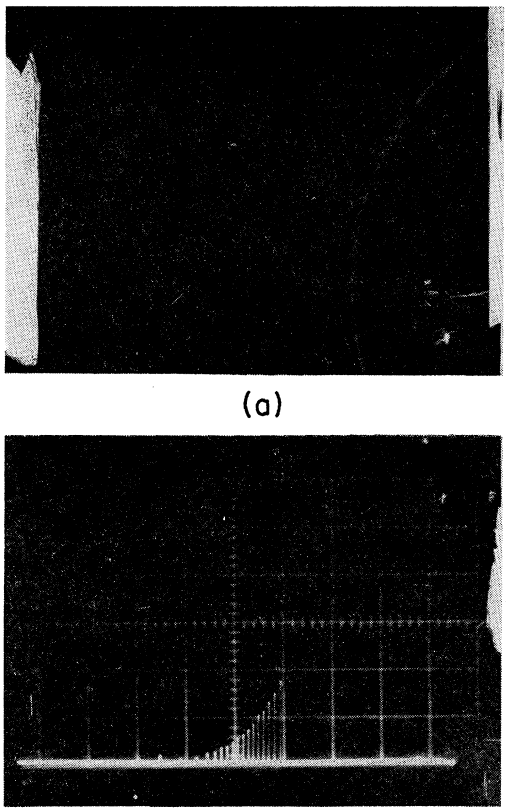

FIG. 3. (a) Fabry-Perot pattern and (b) output intensity of the traveling-wave ruby laser. The separation between Fabry-Perot orders is 1.6 cm^{-1}; scope scale is 100 μsec/cm.

the cavity modes are traveling waves and there is no spatially nonuniform depletion of the inverted population. The device is shown schematically in Fig. 1.

The output was coupled out with an additional quartz prism at one of the 45° reflecting surfaces of the quartz prisms. The output spectrum was analyzed with a 5-cm Fabry-Perot interferometer. The interferometer plates are dielectric coated for 98% reflection and the resolving power is approximately 0.005 cm^{-1}.

The output was further analyzed electronically with a silicon diode photo detector (Philco L4501) to detect any possible beat frequencies between oscillating modes up to the third beat of the fundamental (about 230 Mc/sec). The output power was estimated with the help of a properly calibrated EG&G Lite-Mike.

III. RESULTS

For comparison, we show in Fig. 2 the Fabry-Perot pattern and the time variation of the total intensity of the output of a ruby rod used in a conventional laser setup. The total spectral width of the output is of the order of 1 cm^{-1} [as shown in Fig. 2(a)]. When this same ruby was used in the traveling wave setup as shown in Fig. 1, there was a drastic reduction in the total spectral width, as shown in Fig. 3(a). The separation between successive orders of the Fabry-Perot patterns of Figs. 2(a) and 3(a) are the same. The spiking pattern shown in Fig. 3(b) also shows a drastic improvement. Under similar pumping conditions, with the isolator not in use (no magnetic field) and the 45° passive rotator out of the circuit, results similar to those in Fig. 2 were obtained.[7a]

To show the output characteristics in greater detail, Fig. 4(a) gives the Fabry-Perot pattern with the successive orders separated by 0.1 cm^{-1} which appears to indicate the presence of only one oscillating mode. When the pump was increased much above the threshold (above 25%), two or three oscillating modes could appear, as can be clearly seen in the Fabry-Perot patterns shown in Figs. 5(b) and 5(c), with a mode separation of approximately 0.008 cm^{-1}. The total width even in the case of Fig. 5(c) is still very much smaller than that shown in Fig. 2(a).

When two modes are present the diode detector output contains a beat signal at 230±1 Mc/sec, giving a total laser optical path length of 130 cm. Figure 6(a) shows the total intensity of the single-mode laser output;

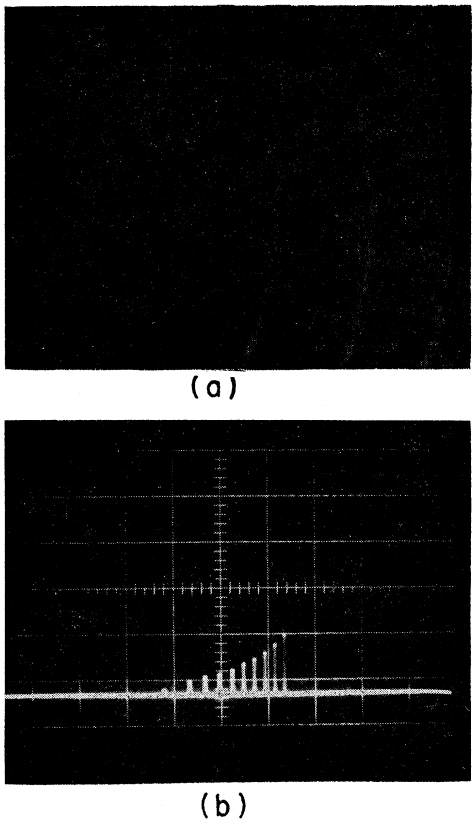

FIG. 4. (a) Fabry-Perot pattern and (b) output intensity of the traveling-wave ruby laser. The separation between Fabry-Perot orders is 0.1 cm^{-1}; scope scale is 50 μsec/cm.

[7a] *Note added in proof.* In the original photos for Fig. 3(a), Fig. 4(a), and Fig. 5(b), the Fabry-Perot patterns are very clear. They cannot be reproduced as clearly here because of production difficulties in engraving and printing.

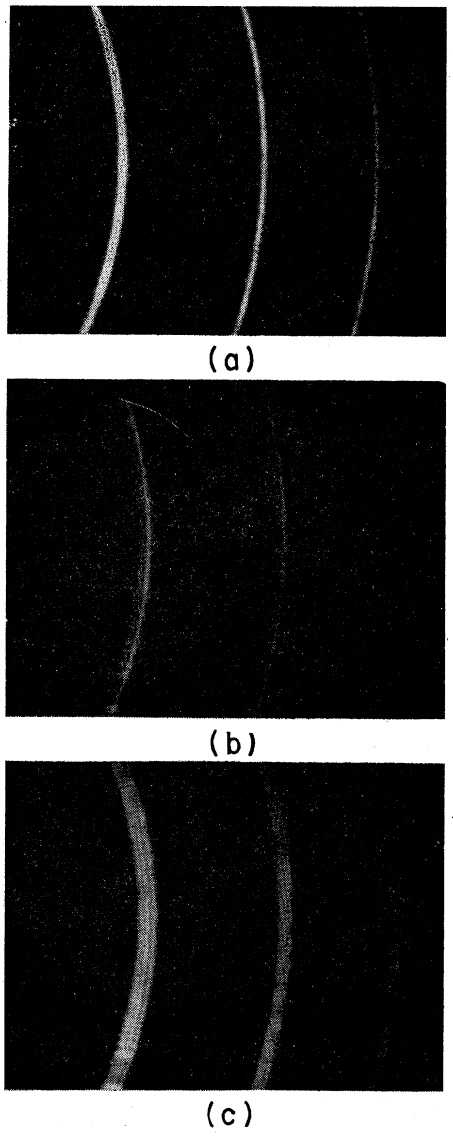

FIG. 5. Fabry-Perot patterns of the traveling-wave laser oscillating in (a) one, (b) two, and (c) three modes. Fabry-Perot orders are separated by 0.1 cm^{-1}.

Fig. 6(b) shows the 230-Mc/sec beat output. No 460-Mc/sec beat was observed. These results show that we have obtained a single-mode oscillation for all practical purposes. The cause of the initial beat at 230 Mc/sec will be discussed in the following section.

The more sensitive diode detection is important if one wants to be sure that there are no weak modes present. Unless extreme care is taken, the Fabry-Perot picture could very often be misleading when the intensities of different modes are very different. As an example, Figs. 7(a) and 7(d) show the results of simultaneous measurements of the total intensity of the laser output, the 230- and 460-Mc/sec beats of the diode output, and the Fabry-Perot pattern of a single shot of the

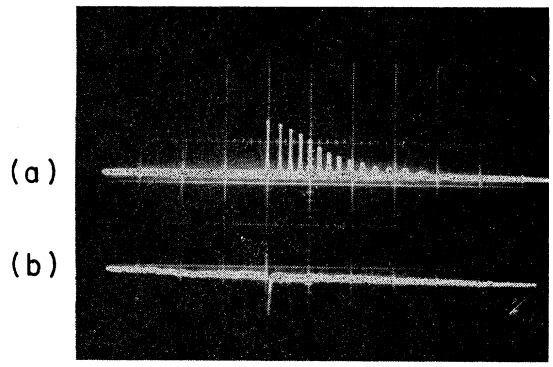

FIG. 6. (a) Total intensity of the laser and (b) the beat signal at 230 Mc/sec in the diode photodetector output; scope scale is 50 μsec/cm.

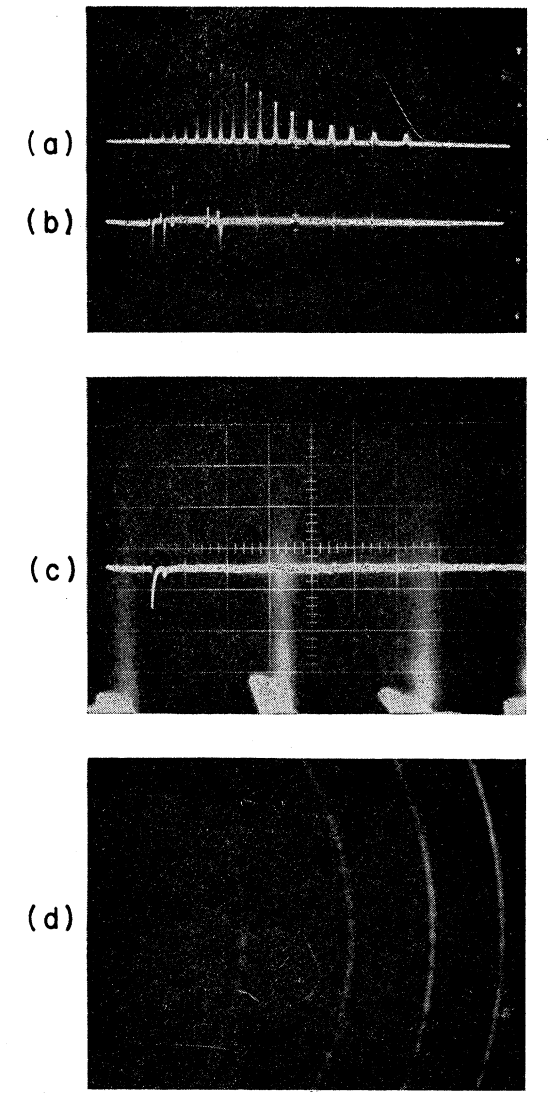

FIG. 7. (a) Total intensity of the laser output, (b) the 230-Mc/sec beat signal, (c) the 460-Mc/sec beat signal, and (d) the Fabry-Perot pattern. Fabry-Perot orders are separated by 0.1 cm^{-1}; scope scale is 50 μsec/cm.

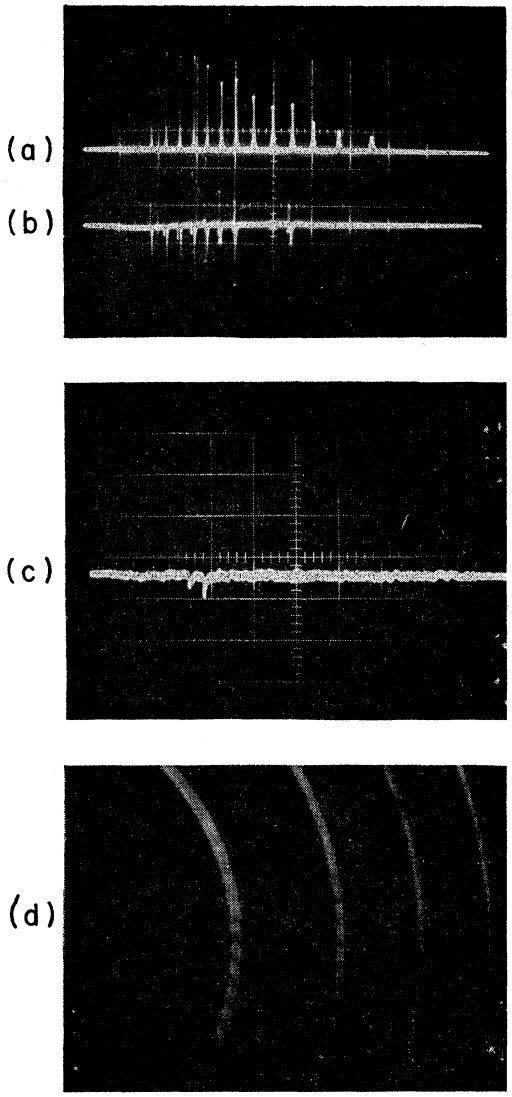

FIG. 8 (a) Total intensity of the laser output, (b) the 230-Mc/sec beat signal, (c) the 460-Mc/sec beat signal, and (d) the Fabry-Perot pattern. Fabry-Perot orders are separated by 0.1 cm^{-1}; scope scale is 50 μsec/cm.

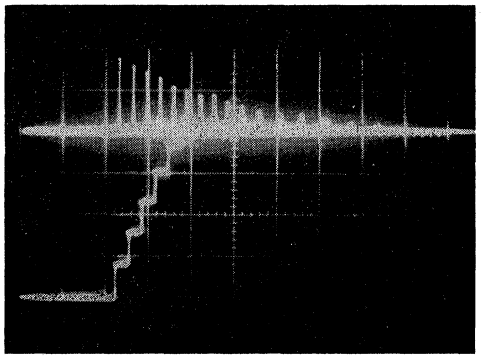

FIG. 9. Upper trace: total intensity; and lower trace: integrated intensity of the laser output.

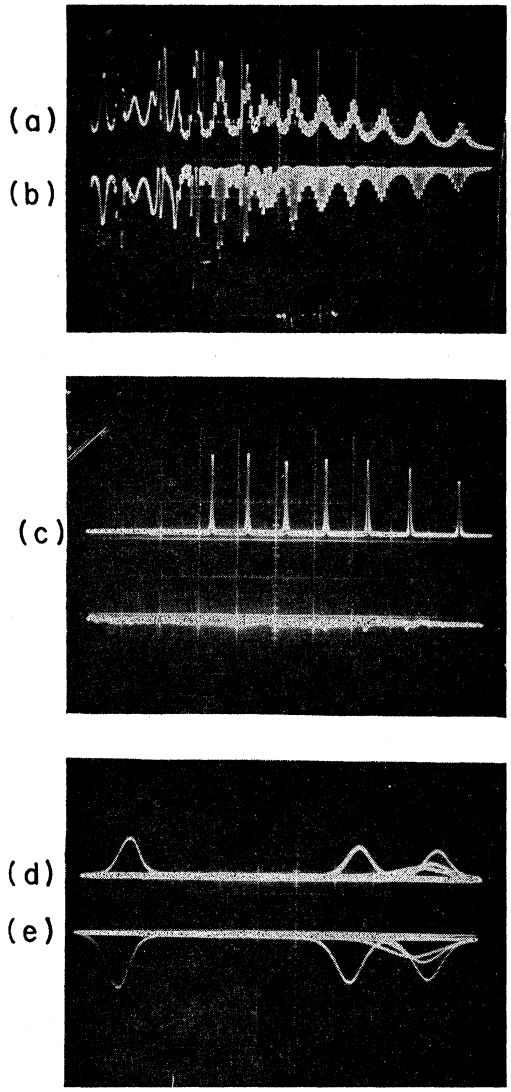

FIG. 10. (a) Phototube response and (b) diode response of the laser output with the optical isolator not in use; scope scale is 20 μsec/cm. (c) Output intensity of the laser with the optical isolator in full use; scope scale is 20 μsec/cm. (d) The phototube response and (e) the diode response of the laser output with the optical isolator in full use; scope scale is 1 μsec/cm.

laser. The diode output shows clearly the presence of more than one mode on several spikes. In Fig. 8, both the Fabry-Perot picture and the diode output give indications of the presence of two or three modes on certain spikes of the same shot.

When the laser was operating under ideal conditions, as indicated by the single-mode output near the threshold, no third beat at 690 Mc/sec has ever been observed even when the laser was pumped quite hard. The diode and the associated electronic circuits were designed to detect readily any beat signals up to 800 Mc/sec.

Figure 9 shows the integrated intensity of a calibrated fraction of the total laser output as measured by the light mike. For this particular shot we estimate the

peak intensity to be approximately 1 kW. We believe that the power output can be greatly increased.

Figures 10(a) and (b) show the phototube response and the much faster diode photodetector response of the output of the laser shown in Fig. 1 with the optical isolator not in use (no magnetic field) and the 45° passive rotator out of the circuit. The scope speed is 20 μsec per division. Beat signals of the order of 1 Mc/sec or less are clearly seen. Beats up to 6 Mc/sec have been observed on several occasions. These could be due to very-low-order transverse modes of the laser. Figure 10(c) shows a similar scope trace of the phototube response of the laser output when the optical isolator was in full use. The sweep speed is 20 μsec. Figures 10(d) and (e) show similar scope traces of the phototube and diode detector responses where the scope scale is 1 μsec per division. There are no beat signals. Since the spike width is of the order of 1 μsec and the beat signals shown in Figs. 10(a) and (b) are of the order of 1 Mc/sec or less, this is expected. It is of interest to note, however, that we have never observed any low-frequency beat signals as one would expect if transverse modes were present in the traveling wave laser when the isolator was in full use. The total response time of the scope and the electronic measuring systems is of the order of 1/30 μsec.

IV. CONCLUSIONS AND ANALYSIS

The results prove that at room temperature the R_1 line of ruby, which is broadened by the two-phonon Raman process,[7] is homogeneously broadened, and the simultaneously oscillating modes in conventional ruby lasers are due to the spatially nonuniform partially depleted inverted population distribution of the Cr^{3+} ions. As a single-mode ruby laser it leaves more to be desired; but a great improvement from the results reported here can still be made as the experimental model built is far from optimum design. The method for achieving single-mode oscillation and getting rid of random spikes in solid-state lasers with appreciable output can be applied to all lasers in which the fluorescence line is homogeneously broadened and the spatial cross relaxation time is long.

To see what additional physical mechanisms may be of importance in the experiment, it may be of interest to consider the experimental results in more detail. Of course, the spectral characteristics of the laser would be influenced by imperfections in the antireflection coatings and other optical components, etc.; but these experimental difficulties can be minimized.

A. Transient Effects

We consider first the spiking characteristics under ideal conditions. Since, in the present experiment, there should ideally be no nonuniform distribution of the inverted population, the transient problem is amenable to analysis with the help of the simple rate equations. According to such a simple single-mode theory, the time between spikes T_S should be approximately[8]

$$T_S \approx [2\pi Q\tau/f(\alpha-1)]^{1/2}, \quad (1)$$

where Q is the cavity quality factor, τ is approximately half the fluorescence lifetime,[9] f is the frequency, and α is a pump parameter defined as

$$\alpha = \frac{\text{Pump power–pump power required for equalizing the populations of the maser states}}{\text{Threshold value–pump power required for equalizing the populations of the maser states}}.$$

In the present experiment, $\tau = 1.5\times10^{-3}$ sec and $f = 4.3\times10^{14}$ sec^{-1}. For an estimated total loss of 25% due to output coupling and losses in all the optical components in the optical path, we obtain an estimated effective Q of 3.6×10^7. α is somewhat hard to estimate since it is difficult to know accurately the pump power required for equalizing the population, but an α of 2 is a reasonable value. Using these values one finds $T_S \approx 28$ μsec, which is in agreement with the experimental values obtained ($\sim$20 to 50 μsec). The damping of the spikes cannot be checked since the observed damping was due to the decay of the pump light.

Even in the ideal situation, although there should be only one steady-state oscillating mode, during the first few spikes in the transient period there can be several oscillating modes. Physically, this is due to the fact that during the transient period the population inversion also oscillates. It could build up temporarily to a level far exceeding the steady-state level, which is equal to the threshold level, thus allowing coherent radiations in modes with higher losses to build up. But these modes die out rather quickly, leaving only the mode with the least loss oscillating. We now proceed to demonstrate this mathematically.

It would be sufficient to consider only the first two modes. In the present case, the simple rate equations approach for the transient behavior of the laser can be used, since there is essentially no spatial variation in the inverted population and all the other conditions for the validity of such a description are satisfied.[10] The required coupled nonlinear rate equations can be written

[8] H. Statz and G. A. deMars, *Quantum Electronics*, edited by C. H. Townes (Columbia University Press, New York, 1960), p. 530.

[9] $1/\tau$ actually should equal $1/\tau_f + g$, where τ_f is the fluorescence time and g is the rate of increase of the population of the upper maser state due to pumping divided by the population of lower maser state. In practice, $g \approx 1/\tau_f$; therefore, $1/\tau \approx 2/\tau_f$.

[10] C. L. Tang, J. Appl. Phys. 34, 2935 (1963); C. R. Willis, Bull. Am. Phys. Soc. 9, 399 (1964).

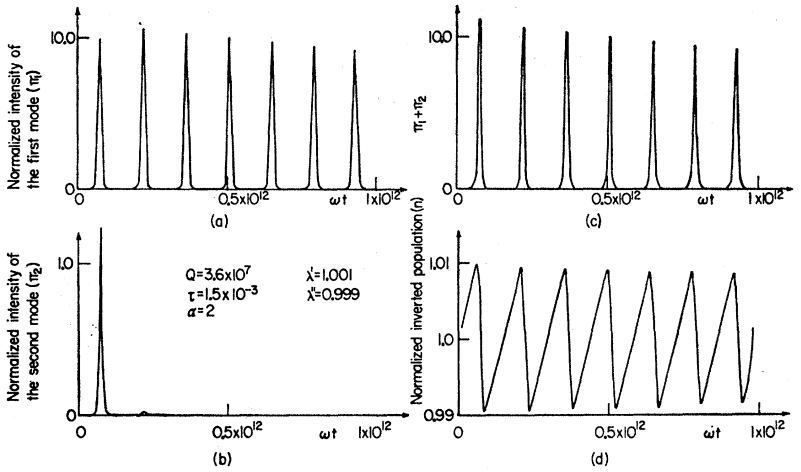

FIG. 11. Calculated transient oscillations of the intensities of (a) the first mode (π_1), (b) the second mode (π_2), (c) $\pi_1+\pi_2$, and (d) the inverted population of the traveling-wave laser.

down at once:

$$\frac{d\pi_1}{dt}=-\frac{\omega}{Q}(1-n)\pi_1, \tag{2}$$

$$\frac{d\pi_2}{dt}=-\frac{\lambda'\omega}{Q}(1-\lambda''n)\pi_2, \tag{3}$$

$$\frac{dn}{dt}=-\frac{n-\alpha}{\tau}+\frac{1-\alpha}{\tau}n(\pi_1+\pi_2), \tag{4}$$

where π_1, π_2, and n are, respectively, the intensities of the first and second modes and the inverted population. They are normalized such that in the steady state:

$$n=1, \quad \pi_1=1, \quad \text{and} \quad \pi_2=0. \tag{5}$$

In Eqs. (2)–(4), α and τ have already been defined previously. Q is the cavity Q for the lowest mode, λ' is the ratio of the cavity Q's of the first and second mode, and λ'' is the ratio of the threshold values of the first and second mode. We have obtained numerical solutions to these equations for a number of typical cases.

The parameters used are again $\tau=1.5\times10^{-3}$ sec, $Q=3.6\times10^7$, and $\alpha=2$. The values of λ' and λ'' are somewhat hard to estimate. How quickly the second oscillating mode dies out during the transient period depends upon these parameters. For example, if we neglect the difference in the Q's ($\lambda'=1$) and assume a fluorescence line of perfect Lorentzian shape with a width of 10 cm^{-1}, for a mode separation of 0.01 cm^{-1} we have $\lambda''=0.999996$. In this case, the intensity of the second mode becomes much less than that of the first mode after nearly twenty spikes. If we use $\lambda''=0.99$, there are only two extremely weak spikes in the second mode before it dies out completely. In the present experiment, due to partial reflections ($\lesssim0.2\%$) at all the reflecting surfaces, the variation in the Q's is probably more important. For an assumed 0.1% change in the Q's, $\lambda'=0.999$; we neglect the line shape factors and assume $\lambda'\lambda''=1$. Figures 11(a)–11(d) give π_1, π_2, $\pi_1+\pi_2$, and n as functions of t obtained by integrating Eqs. (2)–(4) numerically with the help of an IBM-7044 computer. The results show the expected behavior.

B. Thermal Effects

For pulsed lasers, as in the present experiment, the effects of increase in temperature during the laser pulse could be quite important. A more serious effect is the shift of the cavity resonances to longer wavelengths due to the change of index of refraction and the thermal expansion of ruby with temperature. Judging from Fig. 5, for example, the total shift during the entire laser pulse is no more than 100 Mc/sec. The calculated value is about 50 Mc/sec.[11] To avoid this in pulsed lasers, one must stabilize the temperature during the laser pulse or use other compensating schemes such as inserting in the optical path in the cavity a section of optically transparent material with a temperature coefficient of the index of refraction opposite to that of ruby.

Concomitant with the two-phonon broadening of the R_1 line, there is a shift of the line center to the red due to the second-order process in which absorption and emission of phonons of the same frequency occurs.[7] Such a shift is highly temperature-dependent, and during a single laser pulse it could be as much as several hundred Mc/sec.

The effect of this shift on the oscillation frequency of any given laser mode is relatively minor, since the pulling effect is always reduced by the ratio of the cavity width to the fluorescence linewidth. In those cases where the cavity resonances are closely spaced due to a long optical feedback path, it could lead to mode jump-

[11] G. R. Hanes and B. Stoicheff, Nature **195**, 587 (1962). In the present work, this is estimated by two different methods. On the basis of measurements made on similar lasers, the temperature rise during the laser pulse is estimated to be about 0.15°C, giving a shift of about 60 Mc/sec. Interferometric measurement of the change in the optical length of the ruby rod during the pump flash gives a shift of 45 Mc/sec during the laser pulse.

ing. When the fluorescence line moves to a position more or less symmetrical with respect to two cavity modes, both could oscillate. This is believed to be responsible for some of the 230-Mc/sec beat signals observed in our experiment, especially those appearing not at the onset of the laser pulse. This can obviously be avoided by using a shorter optical feedback path. The residual pulling effect can again be compensated in the same way as that for the cavity shift.

At low temperatures ($\lesssim 77°K$), the fluorescence line shape becomes more complicated due to the fact that the $^4A_2$ ground state of Cr^{3+} in Al_2O_3 is actually split by about 0.38 cm^{-1} due to spin-orbit interaction in a crystal field of C_3 symmetry.[12] In addition, as the temperature is reduced, although the total fluorescence linewidth is reduced, the ratio of the temperature-dependent part of the width to the temperature-independent strain broadened width decreases. When the separation between the cavity resonances is larger than the temperature-dependent part but still smaller than the strain broadened part of the total linewidth, one would then expect that the oscillating modes will be able to burn holes into the fluorescence line, and more than one mode will again be able to oscillate as the two-phonon Raman process becomes less and less effective in quenching other oscillating modes. Preliminary experimental results indicate this to be the case, although we have not yet obtained conclusive results due to the difficulties involved in keeping the laser rod at the desired low temperature.

[12] J. E. Geusic, Phys. Rev. **102**, 1252 (1956); A. L. Schawlow, *Advances in Quantum Electronics*, edited by J. R. Singer (Columbia University Press, New York, 1961), p. 232.

ACKNOWLEDGMENT

The assistance of Miss W. Doherty in our numerical work is gratefully acknowledged.

PHYSICAL REVIEW VOLUME 136, NUMBER 1A 5 OCTOBER 1964

Strong Phonon Effects in High-Transition-Temperature Superconductors

A. M. CLOGSTON
Bell Telephone Laboratories, Murray Hill, New Jersey
(Received 23 April 1964)

The high-transition-temperature superconducting compounds V_3Ga and V_3Si have a very large electronic specific heat and strong temperature-dependent susceptibility. These properties are interpreted in terms of a large electron-phonon enhancement of the density of states, and a large exchange enhancement of the susceptibility.

WE have reported previously on some of the unusual properties of the high-temperature superconductors crystallizing in the β-wolfram system.[1,2] These unusual properties include a strongly temperature-dependent susceptibility and Knight shift,[1,2] and a very large low-temperature electronic specific heat.[3] In our original interpretation of these properties, we suggested that the band structure of V_3Ga and V_3Si is such that a high, narrow peak in density of states exists at the Fermi level. We now wish to modify this interpretation. We shall advance a hypothesis below that leads to the conclusion that the susceptibility and specific heat of V_3Ga and V_3Si are strongly affected, respectively, by Coulomb exchange interactions and electron-phonon interactions. The effect of these interactions is to exaggerate the temperature dependence of the susceptibility and to greatly increase the electronic specific heat at low temperatures. In Ref. 2, the temperature-dependent Knight shift has been used to identify a temperature-independent orbital contribution to the sussceptibility of V_3Ga and V_3Si. Various uncertainties place the orbital susceptibility in the range $5.2-7.5\times10^{-4}$ emu/mole. To simplify the considerations that follow we shall adopt the value 7.0×10^{-4} emu/mole as being close to the correct value. The value chosen will not affect the qualitative aspects of the arguments to be made. We shall take χ_{mole} to be the susceptibility of V_3Ga or V_3Si in units of emu per mole due to the spin paramagnetism, and equal to the measured susceptibility minus the orbital susceptibility. We neglect the small Landau diamagnetism. If χ_a is the susceptibility per atom corresponding to χ_{mole}, $\chi_a/2\mu_B^2$ has units of states per erg per atom. In more convenient units we have $\chi_a/2\mu_B^2$ (states per electron volt per atom)$=1.55\times10^4\ \chi_{\text{mole}}$. In Fig. 1 we have plotted $\chi_a/2\mu_B^2$ as a function of temperature for V_3Ga[1] using units of states per electron volt per vanadium atom. We also indicate the density of states at the Fermi level $\eta(E_f)=7.1$ states/eV-atom derived from the low-temperature specific heat.[3]

[1] A. M. Clogston, and V. Jaccarino, Phys. Rev. **121**, 1357 (1961).
[2] A. M. Clogston, A. C. Gossard, V. Jaccarino, and Y. Yafet, Phys. Rev. Letters **9**, 262 (1962).
[3] F. J. Morin and J. P. Maita, Phys. Rev. **129**, 1115 (1963).

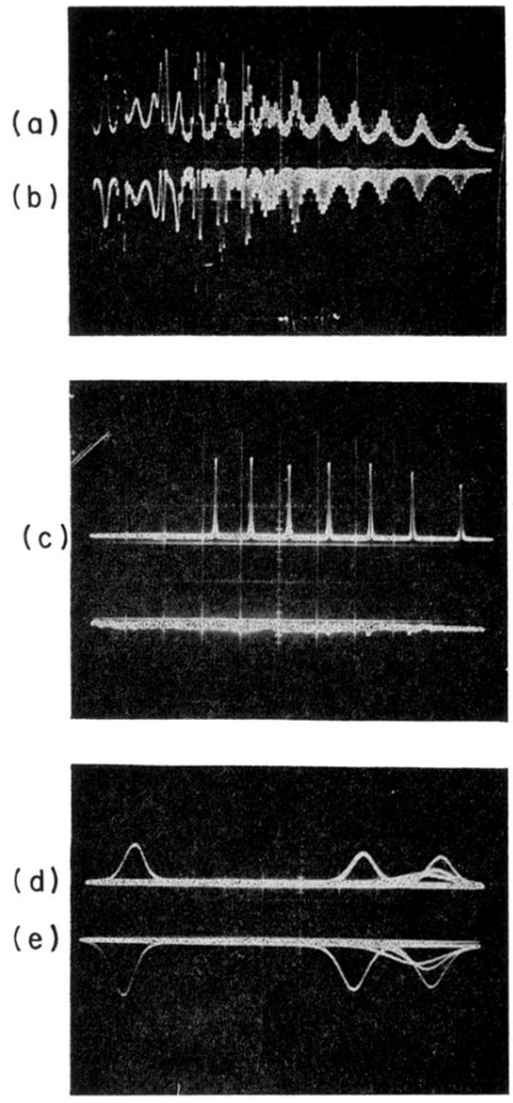

FIG. 10. (a) Phototube response and (b) diode response of the laser output with the optical isolator not in use; scope scale is 20 μsec/cm. (c) Output intensity of the laser with the optical isolator in full use; scope scale is 20 μsec/cm. (d) The phototube response and (e) the diode response of the laser output with the optical isolator in full use; scope scale is 1 μsec/cm.

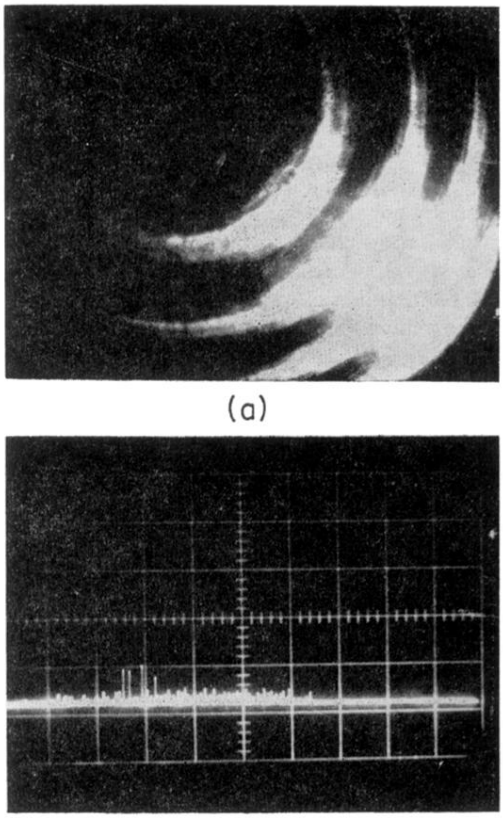

FIG. 2. (a) Fabry-Perot pattern and (b) output intensity of a conventional ruby laser at room temperature. The separation between Fabry-Perot orders is 1.6 cm^{-1}; scope scale is 100 μsec/cm.

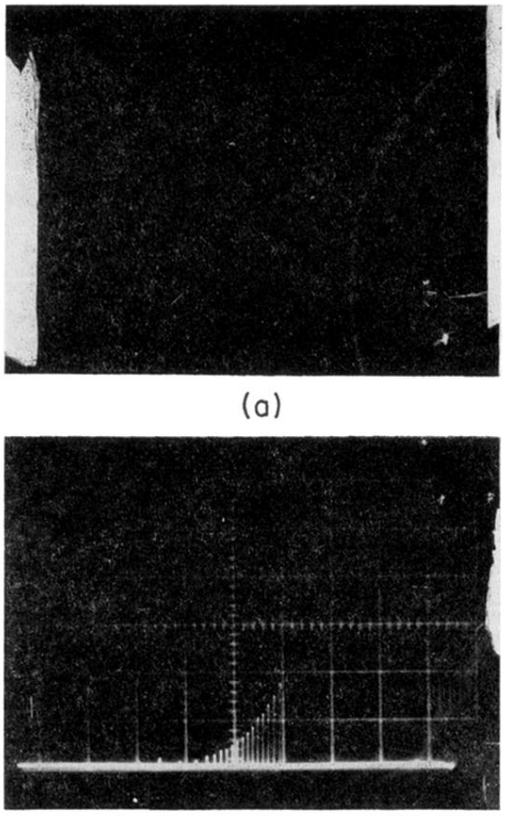

FIG. 3. (a) Fabry-Perot pattern and (b) output intensity of the traveling-wave ruby laser. The separation between Fabry-Perot orders is 1.6 cm^{-1}; scope scale is 100 μsec/cm.

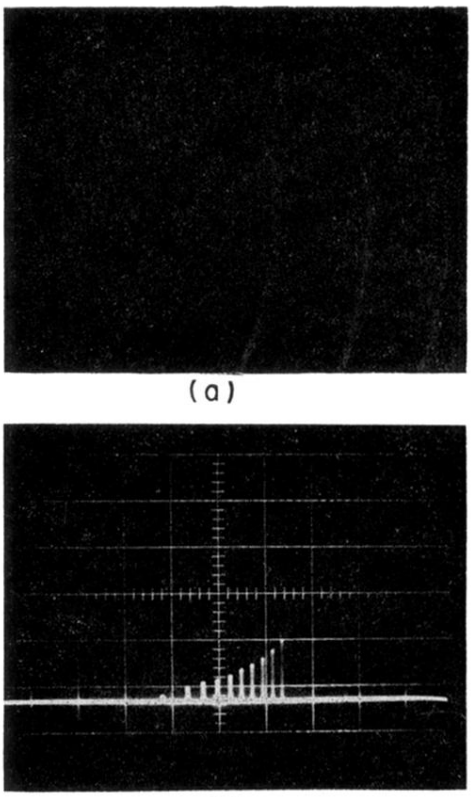

FIG. 4. (a) Fabry-Perot pattern and (b) output intensity of the traveling-wave ruby laser. The separation between Fabry-Perot orders is 0.1 cm^{-1}; scope scale is 50 μsec/cm.

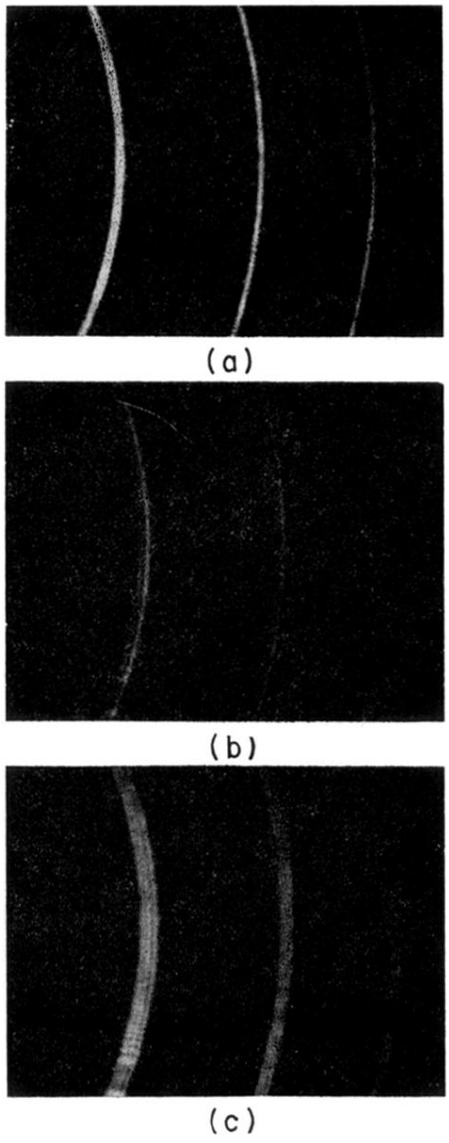

FIG. 5. Fabry-Perot patterns of the traveling-wave laser oscillating in (a) one, (b) two, and (c) three modes. Fabry-Perot orders are separated by 0.1 cm^{-1}.

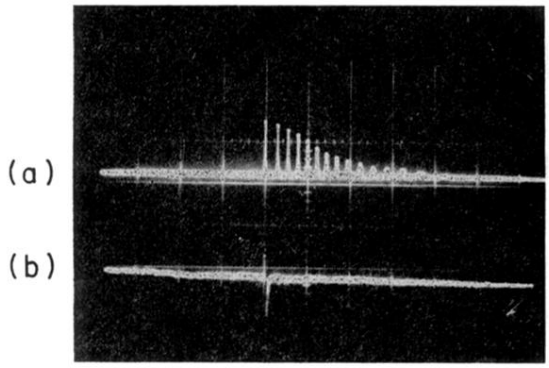

FIG. 6. (a) Total intensity of the laser and (b) the beat signal at 230 Mc/sec in the diode photodetector output; scope scale is 50 μsec/cm.

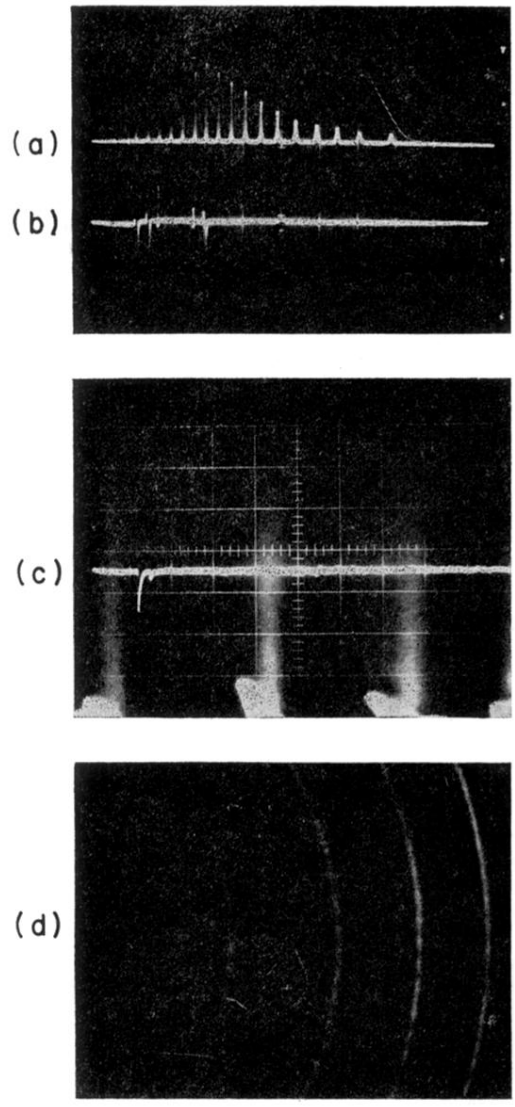

FIG. 7. (a) Total intensity of the laser output, (b) the 230-Mc/sec beat signal, (c) the 460-Mc/sec beat signal, and (d) the Fabry-Perot pattern. Fabry-Perot orders are separated by 0.1 cm^{-1}; scope scale is 50 μsec/cm.

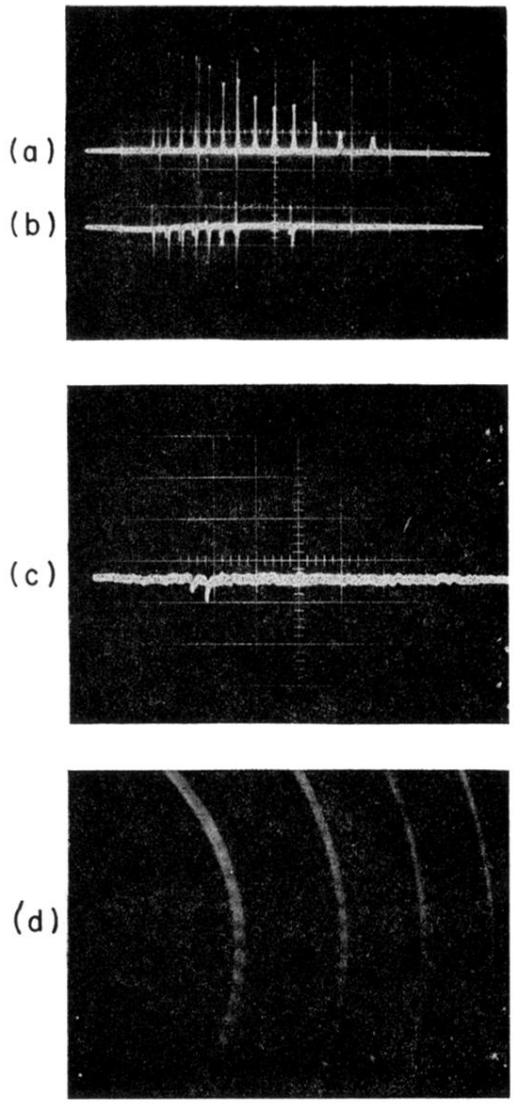

FIG. 8 (a) Total intensity of the laser output, (b) the 230-Mc/sec beat signal, (c) the 460-Mc/sec beat signal, and (d) the Fabry-Perot pattern. Fabry-Perot orders are separated by 0.1 cm^{-1}; scope scale is 50 μsec/cm.

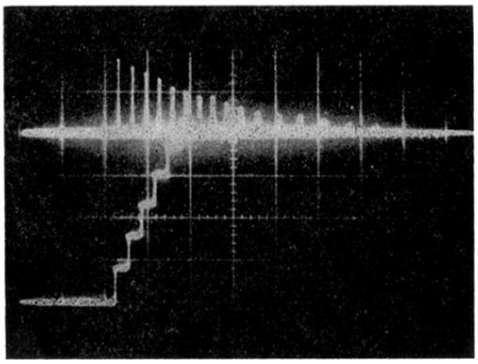

FIG. 9. Upper trace: total intensity; and lower trace: integrated intensity of the laser output.